Use of crop models to evaluate the impact of climate change on wheat irrigation performance and crop yield in the Mediterranean region

RUGIRA Patrick

Abstract— Climate change is a very serious threat to the agricultural sector, and potentially brings new problems for the sustainability of agricultural production systems. This study aims to know the impact of climate change on wheat *(Triticum aestivum* L.), growth management and yield by simulating changes in climate variables using AquaCrop, CROPWAT, and LocClim models, the case study was in the eastern province of the north-west coastal land of Egypt. Testing the equity of the model for experimentation with proposed climate scenarios in this study firstly through enforced temperature gradient (-5 to +5^{o}C) and secondly by using diverse extracted climate normal data of local site reassured the intellectual hint of using the local calibrated AquaCrop model for virtual experimentation. The achieved experience of this study highlights the necessity of using smart agriculture tools and models for setting on-site scheduling of irrigation water that produces actual soil water availability rank versus climate conditions, which would be the ultimate control of both saving water and producing acceptable values of biomass and yield subject to anticipate climate change incidence, which is much more appreciated in Mediterranean land regions.

Index Terms— AquaCrop, climate change, CROPWAT, irrigation, LocClim, model, Wheat,

1 INTRODUCTION

1. INTRODUCTION

McGill et al. (2015) in FAO review on Egypt's wheat sector stated that wheat is by far the most important crop, accounting for almost half of the winter area; about 47% of cultivated winter cropped area grown throughout Egypt, in the Delta region, along the banks of the Nile in Middle Egypt.(Wally & Verdonk, 2016) stated in their report that Egypt's wheat production is on average of 6.43ton/ha.

More productive and sustainable agriculture requires transformations in the management of natural resources and higher efficiency in the use of these resources and inputs for production (McCarthy *et al*. 2011). Despite technological advances, including irrigation systems, the weather is still a key factor in agricultural productivity, as well as soil capability factors and natural communities. The effect of climate on agriculture is related to variability in local climate change than in global climate patterns, in fact, no other sector offers greater synergies between food security and mitigating climate change as agriculture.

It is noteworthy though that seasonal rainfall variation in semi-arid African countries is already large, raising the question whether in the medium-term, farmers will have to cope with anything that they are not already dealing with (FAO, 2009). Irrigation water is gradually becoming scarce, especially in arid and semi-arid regions, hence water-saving, and conservation is essential to support agricultural activities (Garcìa et al 2013). Climate change will have differentiated effects in the countries characterized by different levels of development and which are locating in different climatic zones. (FAO 2010) Declared the presence of considerable knowledge gaps relating to the suitability and use of the production systems and climate-smart practices under varying future climate change scenarios and other biotic and abiotic stresses. Climate-smart agriculture is defined by FAO as agriculture that sustainably increases productivity, resilience (adaptation), mitigation, and enhances achievement of national food security and development goals (CSA, FAO, 2010). Still, many times, technologies, the existing knowledge and inputs have not reached farmers, especially in developing countries (FAO, 2013). (Wiebe et al, 2015) Studied the climate change impacts on agriculture found that without adaptation by the farmers, global crop yields in 2050 would be 6.9% below estimated yields without climate change cereal yields would be lower by as much as 10% in both developed and developing regions. Indeed, and similar to many other countries, Egypt needs a shift in mentality in the way it handles its scarce water resources, as well as minimizing the impact of climate change on crop water consumption.

To study the effects of climate change on agriculture, special models such as those evaluating crop development, yield prediction, and quantities of water or fertilizer consumed, can be employed. The present study involves experimenting with locally calibrated and validated AquaCrop simulation model together with CROPWAT and LocClim programs (after calibrating locality parameters).

The main objective of the project aims at applying, validating and experimenting with FAO models for the interrelated crop and hypothesized local climate scenarios to understand and evaluate the level, the extent and the measures needed to cope

with the impact of the climate change on crop yield and contribute to the management of scarce water resources in the newly reclaimed areas of Egypt based on databases and complementary experimental data. With the following specific objective: 1, implementing ecological concepts in setting assumptions and controls to mitigate effects of climate change (ecological agriculture). 2, connecting between the intensity of exploitation of irrigation water supply with climatic alternations and the availability of its agricultural resources for finally determining/ measuring the state and/or the extent of the current risks of weather events related to climate change. 3, experimenting and enhancing the traditional use of measured weather parameters in farm management (using enforced and extracted climate normal scenarios) by considering the masked indirect effects of weather on physiological processes including the levels of crop production, yield, water use, and water productivity. 4, establishing the appropriate integrated crop-water management scenarios to reduce Egypt's vulnerability regarding scarcity of water under climate change scenarios.

2. MATERIALS AND METHODS

2.1 Field experiments

The study area is located at 30.71°N and 30.74°E and 11 m of elevation in the eastern province of the north-west coastal land of Egypt at Nouberia (Esraa site). In general, the Mediterranean coastal land of Egypt belongs to the dry arid climatic zone. It experiences its hottest temperature and dry weather during the summer months (June to August) up to an average maximum of 26-28°C and the coldest month is January where the minimum and maximum temperatures are 6.2 and 19.5. The average annual amount of rainfall was found to be 53 mm/year with average potential evapotranspiration rates of 131.9167 mm/month. The soil of the study site was characterized as a loamy sand soil, the climate data for the baseline period of 20 years were collected in the nearest meteorological station which is Tahrir station.

2.2 ata collection

According to Doorenbos and Kassam,(1979; FAO document 33), the phonological phases for wheat crop worldwide are distinguished into seedling 10-15days after sowing, followed by early vegetative (tillers) 15-25days, then late vegetative (head formation) 40-50 days, and flowering stage 15-20days, followed by early fruiting for 30-35days, and ending by grain maturation 10-15days; all added to a crop cycle length of 120-160 days. These values were used as a reference guide to set appropriate sampling dates of the local crop in the present study based on field observations. All plant and soil samples were collected at mid-time of each of the revised phonological stages of the crop except for the final phase (grain maturation), which was sampled at its end.

Soil samples from 1-30, 30-60, and 60-90 cm depths were collected. The soil samples were analysed for soil texture, saturation, field capacity, welting point, available water, infiltration rate, soil bulk density, PH, nitrogen concentration electric conductivity, the concentration of soil soluble cations (Ca++, Mg++, K+, Na+) and anions (SO4--, HCO3-, Cl-), and available micro and macronutrients (Fe, Cu, Mn, Zn, N, P, and K). The result of various properties of soil has been summarized in (table 1).

Table 1. Soil texture classes (%) for different soli horizons and Hydraulic parameters for different soil horizons.

Depth	Sand	Silt	Clay	Soil texture	Saturation	Field capacity	Welting point	Available water
0-30	85	10	5	Loamy sand	23.4	12.94	5.69	7.25
30-60	87	8	5		21.01	11.37	4.18	7.19
60-90	87	8	5		27.87	16.39	7.34	9.19
Average 0-60 cm	86	9	5		22.21	12.16	4.94	7.22
Average 0-90 cm	86.3	8.7	5.0		26.77	15.07	6.37	8.7
Infiltration rate = 1.4cm/h and average soil bulk density = 1.4 g/cm								

Plant density was determined by using a 25×25cm² wooden quadrate randomly thrown, at the end of grain maturation phase, all plant individuals (involving attached tillers) within random 25×25cm² quadrate were collected for counting the number of spikes per individual, air dry weight of each plant individual excluding spikes, which were separated into grains and straw air-dry weight. Plant samples were randomly selected to measure growth parameters the average measurements of selected growth stages in the present study is presented as mean and '95%' confidence limits in (Table 2). These results are used to verify the biomass model outputs. All yield components' measurements are recorded only at harvest stage as presented in (Table 2). Yield per air-dry weight percentage is used to calibrate the model input for harvest index, while grains weight is used to verify simulation output for yield production.

Table 2. The average measurements of composite sampled wheat plants (mean & 95% confidence limits) from the permanent sampling plots.

Stage (Date)	Maximum root depth (cm)	Shoot height (cm)	Longest leaf length (cm/ind.)	Widest leaf width (cm/ind.)	Fresh weight (gm. /ind.)	Total area of green leaves (cm^2/ ind.)	L A I	Air-dry weight (ton/ha)	No of plants (ind/m^2)
Establishment (6-Dec-2019)	11.71± 0.73	10.38 ± 1.3	7.22 ± 2.2	0.5 ± 0.08	0.23 ± 0.05	9.88 ± 2.33	0.3 ± 0.08	0.35 ± 0.06	305 ± 63
Early vegetative (19-Dec-2019)	24 ± 0	15.9 ± 0.94	13.5 ± 0.76	0.79 ± 0.22	0.68 ± 0.2	37. 7 ± 15.9	1.77 ± 0.79	0.83 ± 0.21	452 ± 77
Late vegetative) (15-Jan-2020)	19.4 ± 1.44	25.12 ± 3.1	16.12 ± 1.4	1.25 ± 0.41	2.73 ± 0.48	96.1 ± 18.5	3.52 ± 1.03	1.77 ± 0.34	345 ± 52
Flowering (26-Feb-2020)	43 ± 0	86.6 ± 4.4	21.7 ± 0.79	1.47 ± 0.06	12.83 ± 2.01	140.4 ± 35.5	4.32 ± 1.22	9.02 ± 0.91	309 ± 26
Fruiting (31-Mar-2020)	41.2 ± 3.02	100 ± 4.86	20.88 ± 1	1.54 ± 0.06	17.8 ± 2.17	81.75 ± 6.0	3.52 ± 0.52	25.32± 4.04	431 ± 55
Grain maturation (23-Apr-2020)	42.4 ± 4.41	0 ± 0	NA	NA	0 ± 0	NA	NA	20.12 ± 2.99	301 ± 32

Grain maturation (23-Apr-2020); No of spikes(ind./m^2)=419±78, Wt. spikes(gm/m^2)=1112±162,Wtgrains(gm/m^2)=845±109,Straw(gm/m^2)= 1160±202, Average yield(Ton/ha)=8.5±1.1, yield/Air dry (%)=42.5±2.1
NA= Not applicable

2.3 Quantity and scheduling of supplementary irrigation

The pilot site was controlled by the implementation of the manually calculated irrigation amount and schedule using long-term historical average climate data while applying the normally practiced fertilization schemes at different crop development stages. The sprinkler irrigation system efficiencies at the pilot site were evaluated in-situ using the fixed grid can catch test (Merrian *et al*.,1980). Irrigation scheduling involves determining both timing of irrigation and quantity of water to apply. Establishing irrigation scheduling requires knowledge about water balance components. Scheduling irrigation should start when soil water content drops below 50% of the total available soil moisture(ICID/FAO, 1995). Therefore, irrigation is scheduled after a fraction of the soil water in the plant root zone has been depleted. For example: a loamy sand soil holds 87 mm of water per 1m depth of soil at field capacity, and if the irrigated plant root zone depth is set to 0.65 m, while an irrigation is to be scheduled when 50% of the soil water in the root zone has been depleted, then the amount of irrigation (water depth, D) is calculated (D = 87 mm × 0.65 m soil depth=56.6 mm). Amount of water need to be applied when soil water drops below 50% is thus 28.3 mm (= 50 % × 56.6 mm).

2.4

2.5 MODELS CALIBRATION AND VERIFICATION

2.5.1 Climate variables

New *LocClim* 1.1 is a software program and database that provides estimates of average climatic conditions of selected locations, the program includes the current updated version of the FAOCLIM database of almost 30,000 stations worldwide, but users can also process their data (FAO. climpag 2020). The data was obtained from national metrological services, and recalculated by FAO based on time (Grieser *et al*. 2006).

The program was set to extract data from the nearest climate stations, that includes all required climate elements and positioned in the middle of the study area with acceptable altitude. The climate normal using long-term 20 years from year 2000, average of metrological elements for the selected station is required as driving decades input to the crop and irrigation model used in the present study and is produced using FAO New LocClim program. Steps of climate data extraction from New LocClim are extracted climate data as decades' values have been used as input to CROPWAT and AquaCrop models.

2.5.2 Irrigation schemes

CROPWAT 8.0 is a decision support tool developed by the Land and Water Development Division of FAO (CROPWAT Software, FAO,2018). It can calculate crop water and irrigation requirements based on soil, climate, and crop parameters data. Furthermore, the program allows the development of irrigation schedules for different management conditions and the calculation of scheme water supply for varying crop patterns (FAO. Water for Sustainable Food and Agriculture,2017). It can also evaluate farmers' irrigation practices and estimate crop performance under both rained and irrigated condition (FAO,2014).

Three irrigation parameters are verified to fit simulation runs to the field conditions. The first concerns the irrigation scheduling parameters where the measured irrigation efficiency is evaluated as 85%. The second controls a trigger of irrigation events that are assigned to irrigate below or above critical depletion (specifically at 50% of critical depletion). The third one controls the amount of irrigation, which is set by default to refill soil water to 100% of field capacity. The calibration of the crop coefficients (Kc) that relate the crop phases to their corresponding water needs required stepwise experimentation interchanging information among AquaCrop and CROPWAT programs. Thus, combinations of crop coefficients (Kc) were tried as input to CROPWAT program to find the corresponding irrigation schedule, which is then tested as input to AquaCrop program, to test the least amount of needed irrigation

that produces acceptable yield performance compared to field measures and extract the corresponding crop phases.
The AquaCrop model version 5.0 used in this study includes fifty-five parameters that define the crop physiological and developmental responses to environmental factors as well as soil water relationship and salinity stresses, soil textural classes along with hydraulic soil parameters are used for calibration and verification of soil water dynamics in Aquacrop model.

2.6 Calibration parameters

Parameters and variables were calibrated according to field observations and the measured data. The methods used to determine values for calibrating the non-conservative soil and crop parameters and variables were dependent on the field observations and the measured data as demonstrated in the following set of evaluations; Day after sawing (at which simulation starts) as recorded in field sites, plant density which controls initial canopy cover was determined as:

$$(Average\ Wt.of\ grain = \frac{wt\ of\ 100\ gram}{100})$$

$$(No\ of\ \frac{grain}{ha} = \frac{wt\ of\ grain\ sawen\ per\ ha}{average\ Wt.of\ grain})$$

while considering germination percent and plant density at establishment and at harvest stages respectively.

Canopy expansion was calculated from 'LAI' values during different phonological stages as [Canopy cover at stage A = (LAI in stage A/LAI in late vegetative stage) *100]. It is also affected by growing day degrees (GDD) value at maximum canopy cover, Maximum effective rooting depth (Z_x) was estimated from root expansion from field observations on root length and used irrigation scheduled, Average root zone expansion depended on the maximum effective rooting depth and GDD value of maximum root depth, Maximum root extraction term (S_x) (S_x top ¼ and S_x bottom ¼) changed in the model according to water extraction pattern (which remains as default) and Maximum effective rooting depth, Normalized biomass water productivity WP* (WP normalized for ET_o and air CO_2 concentration [tone/ha or kg/m^2]) was calculated from biomass production at the yield formation stage.

$$WP = \frac{fresh\ wt\left(\frac{g}{m2}\right)at\ yield\ formation\ stage}{Total\ ETc(mm)}$$

Reference harvest index was obtained from field observations and calculated as

$$HI = \frac{yield\ kg/m2}{biomass\ kg/m2}$$

Soil water stress on canopy expansion, stomatal closure, and early canopy senescence calibrated according to prevailing arid climate condition at study area, Base and upper temperature were changed according to climatic data obtained from New *LocClim* by taking the lowest minimum temperature (base) and highest temperature (upper) recorded along the growing cycle period from the extracted daily climatic values, Cold stress on biomass and pollination calibrated according to local condition as the minimum temperature did not decrease than 5^{o}C, Calendar and GDD were calibrated after testing many simulations run versus recorded field data, Threshold of green canopy cover was calibrated according to the number of green leaves and leaf area at yield formation stage, Minimal soil water for germination was calibrated according to total available water (TAW)and permanent welting point (PWP).

2.7 Climate change scenarios' model experimentation

2.7.1 Composing climate files

Hypothesized high maximum and minimum temperature (^{o}C) is performed by adding 2^{o}C to corresponding temperature values extracted from New LocClim while low-temperature regime by subtracting 2^{o}C from the same corresponding values. Double rain, half rain, and zero rain values are calculated and used in combination with high and low-temperature scenarios. High ETo is calculated by CROPWAT model using high maximum and minimum temperature while low ETo is calculated using low maximum and minimum temperature regime, considering unchanged extracted New LocClim values of humidity (as % or vapor pressure KPa), wind speed (Km/day), the sunshine (h% of day length or fraction of day length)(FAO. Agroclimatic tools, 2005).

Accordingly, six climate scenarios were hypothesized by preparing required combining climate files as follows: High climate (high temperature, ETo, and Double rain), high climate normal rain (High temperature, ETo, and Normal rain), high climate zero rain (High temperature, ETo, and No rain), low climate (low temperature, ETo, and Half rain), low climate normal rain (low temperature, ETo, and Normal rain) and Low climate double rain (Low temperature, ETo, and Double rain).Accordingly, six climate scenarios were hypothesized by preparing required combining climate files as follows: High climate (high temperature, ET_o, and Double rain), high climate normal rain (high temperature, ET_o, and Normal rain), high climate zero rain (High temperature, ET_o, and No rain), low climate (low temperature, ET_o, and Half rain), low climate normal rain (low temperature, ET_o, and Normal rain), and low climate double rain (low temperature, ET_o, and Double rain).

2.7.2 Experimentation with scenarios and scenarios solving

Proposed climate change scenarios are practiced using the

following steps; Running of scenario program in AquaCrop model using net optimum irrigation amount (370 mm) and schedule produced by CROPWAT program (calculated by applying all optimum conditions for crop, plant and soil parameters and variables at normal climate). Crop stages periods are assigned default values of '17, 63, 35, and 34 days' for initial, canopy development, mid-season, and late-season stages respectively (FAO-56). The total irrigation period is set for 149 days, Obtaining from the previous AquaCrop model simulation runs a new set of crop growth stages periods (16, 53, 38 and 37 days) with a total irrigation period of 144 days, Using these new crop growth stages periods and proposed ETo in CROPWAT to calculate new irrigation quantity and schedule for iteration with AquaCrop model, Running of scenario program in AquaCrop model using obtained irrigation file (336 mm) and total irrigation period of 144 days. This run shows excess water at a late stage and beyond, Crop stages periods must be decreased to calibrate CROPWAT irrigation scheduling, obtaining a new crop cycle length using high climate scenario (137 days). Thus, calibrate FAO-56 stages length according to crop cycle (137days) and not crop calendar (144 days) by decreasing maturity stage length in AquaCrop, Assigning new crop stages length (16, 53, 38 and 30) with total irrigation period of 137 days into CROPWAT iteration to obtain calibrated irrigation schedule with no excess water, running of scenario program in AquaCrop model using obtained irrigation (313 mm) with total irrigation period of 137 days. This run shows no excess water.

3. RESULTS

3.1 Plant measurements

Measured crop data are used to extrapolate the interrelations between LAI, soil moisture level, and yield as a function of air-dry weight during the developmental stages (Table 3 and Figure 1). Observed results are used to calibrate the model parameter for green canopy cover percentage and time to start senescence. In addition, the ratio of the number of yellow leaves to the total number of leaves (14, 39, and 75% for late vegetative, flowering and fruiting stages, respectively) is used to calibrate the model senescence time. The extrapolated relations indicate high correlation coefficients of at least 0.98. Those can also be obviously related to the regressed trend of change in calculated growth rate values (R^2 = 0.99) extracted from produced biomass at the different crop's growth stages (Figure 2). Moreover, the calculated canopy cover and senescence percentages are used as model input controls, while the calculated soil moisture content for assigned root depth at each growth stage is used to verify simulated soil moisture distribution.

Table 3. Average crop data of composite plant

Stage (Date)	Days after sowing	Moisture percentage (air-dry)	Yield (gm./m²)	Growth rate (gm./day)	Canopy cover (%)	No. Green leaves (leaf / m²)	Senescence "yellow/total leaves" (%)	Soil moisture content (mm)
Establishment (6-Dec-2019)	16	0.96	0	2.18	6.9	751.28	0.000	74.25
Early vegetative (19-Dec-2019)	29	0.95	0	3.68	40.8	1623.72	0.000	57.78
Late vegetative (15-Jan-2020)	56	3.21	0	3.48	81.5	2447.70	14.043	59.35
Flowering (26-Feb-2020)	98	9.38	0	17.27	100.0	2471.94	38.922	56.17
Fruiting (31-Mar-2020)	131	7.07	0	35.11	85.5	1042.09	74.631	49.43
Grain maturation (23-Apr-2020)	154	7.76	845	0.00	70.0	0.00	100.000	Harvest

** Soil moisture content (mm water) was calculated from measured "tensiometer" values (k Pascal) converted to bars & calibrated by the experimental PF curve for soil moisture characteristic*

Figure 1. Variation of crop measures during different crop stages.

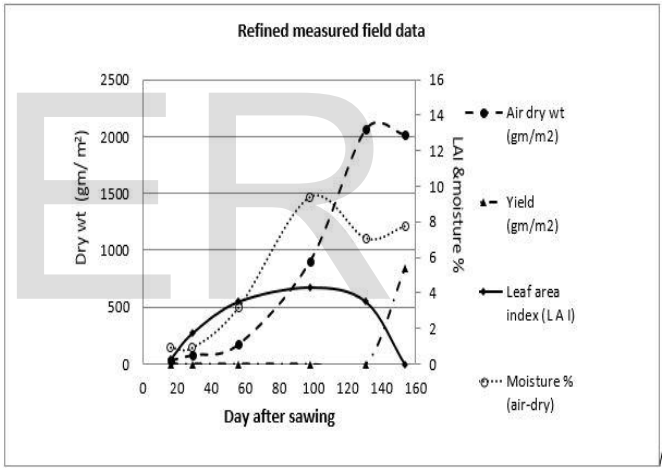

Figure 2. Regression analysis of refined crop biomass and calculated growth rates during the different crop stages.

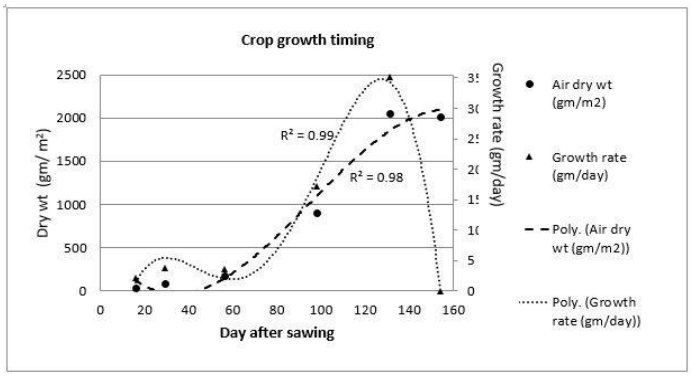

3.2 irrigation

the calibration of the crop coefficients (kc) that relate the crop phases to their corresponding water needs required stepwise experimentation interchanging information among aquacrop and cropwat programs. the selected least irrigation amount that produced acceptably is obtained for 'kc 0.5' for the initial stage and using a value of '1.07' for mid-stage. accordingly, this last combination of crop coefficients (kc: 0.5, 1.07, 0.25) is used to evaluate irrigation needs, and when used the crop consumes 369.9 mm water producing 6.680ton/ha grains yield associated with low water stress on canopy expansion of 1%.

3.3 CALIBRATING A LOCAL MODEL AND ASSOCIATED APPLIED PROGRAMS

The aim of this procedure is to implement the locally calibrated controls and parameters in the present study to verify calibrated models' structures that produce statistically acceptable simulation outputs compared to actual field observations. This would provide a solid reference base for experimentation using different projected scenarios.

3.3.1. Simulation output information

Three simulation runs of AquaCrop model were executed using different irrigation sets including one for the actual field practice amount that was applied using 39 irrigation events under 85% irrigation efficiency. The other two runs were applied for the controlled CROPWAT scheduled output of both under 100% irrigation efficiency (net irrigation; Figure 3) and under actual 85% irrigation efficiency (gross irrigation) using 25 irrigation events. The calculation of the average daily values supported by 95% confidence limits of simulation output of the run using 100% irrigation efficiency for the involved crop within the different development stages considered by the model are presented in (Table 4).

Figure 3. Crop's net and gross irrigation amounts along the suggested schedule (days after sawing) for wheat.

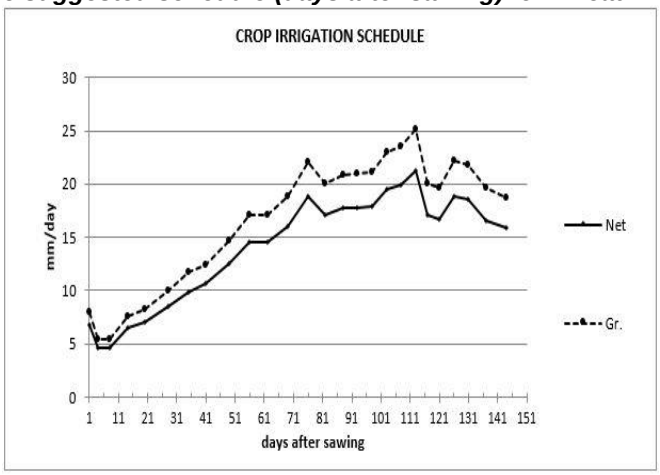

Table 4. A summary of "AquaCrop" model output calculated as average daily values of crop within the different development stages (Mean ± 95% confidence limits).

Stage (range of days)	Growing degrees (GD °C-day)	Effective rooting depth (Z m)	Green total Canopy Cover (CC %)	Cumulative biomass produced (ton/ha)	Adjusted Harvest Index (HI %)	Yield Part (HI x Biomass, ton/ha)	yield part WP (kg/m³ water ET)
1 (1-7)	16.46 ± 0.27	0.3 ± 0	0.71 ± 1.75	0 ± 0	0 ± 0	0 ± 0	0 ± 0
2 (8-70)	13.49 ± 0.27	0.53 ± 0.03	55.03 ± 8.16	2.47 ± 0.53	0 ± 0	0 ± 0	0 ± 0
3 (71-89)	13 ± 0.11	0.65 ± 0	92.96 ± 0.28	8.25 ± 0.43	2.17 ± 0.7	0.19 ± 0.07	0.1 ± 0.03
4 (90-159)	17.14 ± 0.56	0.65 ± 0	78.5 ± 5.86	14.68 ± 0.6	23.53 ± 2.61	3.72 ± 0.51	0.97 ± 0.1
at Harvest	21.20	0.65	0.00	17.49	38.20	6.68	1.51

Stages are: 1; emergence, 2; vegetative stage, 3; flowering stage, and 4; yield formation and ripening.

The relationships between the simulated daily values of 'CC%' and the soil water contents (calculated as moving average of simulated values per decade) at depths of five, fifteen and thirty-five centimeters are clarified by (Figure 4). The soil water content at the second depth (15 cm) displays more or less an intermediary role among the two other soil depths, however, it exposed bouncing pattern during the vegetative and flowering stages related to the active root zone and water input events.

In this respect, a summary of the calculated average daily values supported by 95% confidence limits of water content in the effective root zone within the different development stages is presented in (Table 5). This is evident from the plotted simulated daily values presented in (Figure 5), which also demonstrates the previously stated bouncing pattern during crop growth stages reflecting the water input schedule events.

Figure 4. Crop development simulated daily values in relation to soil water content at various depths (moving average simulated values per decade).

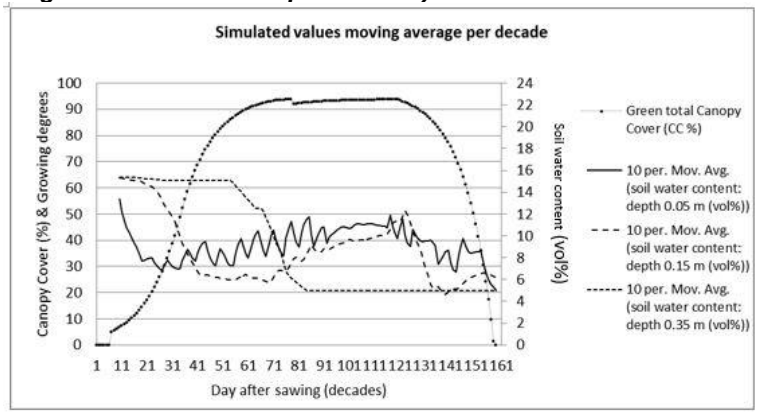

Table 5. A summary of "AquaCrop" model output of average daily value of water content in effective root zone at the different development stages (Z_{rx} = 0.65m) (Mean ± 95% confidence limits).

Stages (days after sawing)	Effective rooting depth Z (m)	Water content (mm)	at upper threshold for leaf expansion (mm)	at upper threshold for early canopy senescence (mm)	at permanent wilting point (mm)	at field capacity (mm)
1 (1-7)	0.3 ± 0	45.2 ± 2.92	37.17 ± 0.8	25.51 ± 0.45	19.2 ± 0	45.3 ± 0
2 (8-70)	0.53 ± 0.03	63.84 ± 2.28	61.82 ± 3.18	42.84 ± 2.2	33.81 ± 1.72	79.78 ± 4.05
3 (71-89)	0.65 ± 0	67.04 ± 2.5	77.12 ± 0.13	53.33 ± 0.08	41.6 ± 0	98.2 ± 0
4 (90-159)	0.65 ± 0	61.66 ± 2.28	80.29 ± 0.38	55.21 ± 0.23	41.6 ± 0	98.2 ± 0
at Harvest	0.65	46.90	83.00	56.80	41.60	98.20

Figure 5. Water content in soil profile and root zone (0.65 m) simulated daily values

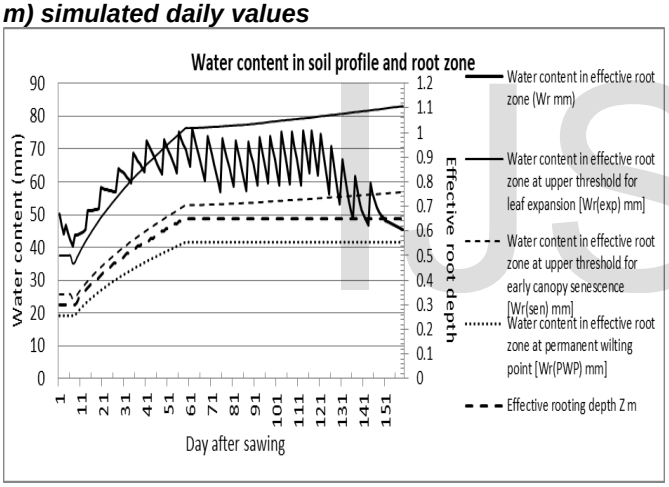

Trends in daily simulated values of crop production calculated as cumulative biomass produced for each crop development stage and it's corresponding calculated growth rates are plotted as scatter points for stages together with a third-order polynomial curve fitting selected based on the coefficient of determination value (R^2) for each of them that are graphed in (Figure 6). For comparison, a graph of the corresponding reworked field observations data collected at specific days and expected to represent the development stages of the crop is presented in (Figure 7). The comparison among those figures reveals acceptable consistency in development pattern of simulated and refined measured cumulative biomass (gm/m2) as well as that of calculated crop growth rates (gm/day) supported by quite high associations among original and predicted values; R^2 ranges between 0.8 and 1.0 for any of them.

On the other hand, the model results regarding the water gain show a balance between irrigation water, rainfall, water infiltration, and drainage quantities (Table 6 & Figure 8). Initially, the daily infiltrated water in the soil is the result of added irrigation amount and the received amount of rainfall as no run-off is considered (was set in calibrated model controls). Both emergence and flowering stages exhibit the higher value of 95% confidence limits for infiltration rate (2.11 ± 2.76 & 3.14 ± 3.25 respectively) compared to the other two stages, which apparently is a reflection of variability in irrigation quantities.

The evaluation of the simulation run output using the actual 85% irrigation efficiency (gross irrigation) is performed by comparing it with the simulation output for the actual field practice irrigation amount. Accordingly, the calculated total water inputs applied and simulated gross irrigation have close values of about 488 and 478 mm, respectively (Figure 9). The calculated crop water needed (the sum of crop evaporation and transpiration) for applied and gross irrigation are similar to a value of about 456mm (Figure 10).

Figure 6. Trends in simulated value of crop production and calculated growth rate

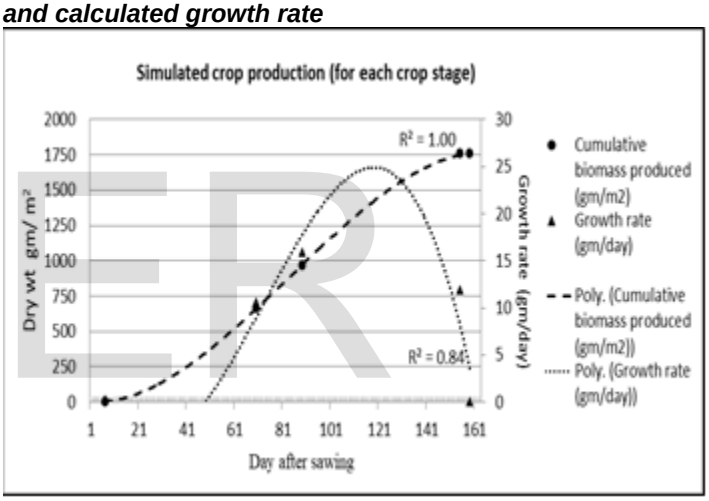

Figure 7. Trends in measured field value of crop production and calculated growth rate

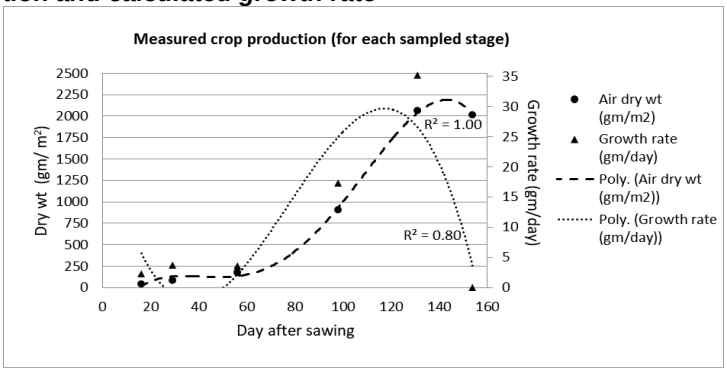

Table 6. A summary of "*AquaCrop*" model output of average daily value of soil water balance at the different development stages (Mean ± 95% confidence limits).

Stages (days after sawing)	Water content in total soil profile "1.2m" [$WC_{1.2m}$ mm]	Rainfall (mm/day)	Water applied by irrigation (Irri. mm/day)	Infiltrated water in soil profile (Infilt. mm/day)	Drain (mm/day)	Soil evaporation (E mm/day)	Total transpiration of crop (Tr mm/day)	Evapotranspiration (ET mm/day)
1 (1-7)	181.91 ± 2.86	0.4 ± 0	1.71 ± 2.76	2.11 ± 2.76	0.71 ± 0.36	1.93 ± 0.21	0.03 ± 0.07	1.97 ± 0.17
2 (8-70)	165.44 ± 2.23	0.37 ± 0.01	1.63 ± 1.02	2 ± 1.02	0.11 ± 0.01	0.51 ± 0.12	1.7 ± 0.23	2.21 ± 0.13
3 (71-89)	150.23 ± 2.51	0.3 ± 0	2.84 ± 3.25	3.14 ± 3.25	0.1 ± 0	0.06 ± 0.02	3.09 ± 0.06	3.15 ± 0.06
4 (90-159)	144.8 ± 2.28	0.13 ± 0.01	2.87 ± 1.6	2.99 ± 1.61	0.1 ± 0	0.14 ± 0.02	3.13 ± 0.36	3.26 ± 0.35
at Harvest	130.00	0.10	0.00	0.00	0.10	0.20	0.00	0.20

The resulting crop cumulative water balance shows at the one hand a surplus of about 32mm for applied and 21mm for gross irrigation attributed mainly to the difference in the total amount of irrigation of about 10 mm. On the other hand, the net irrigation (370 mm, 100% efficiency) shows a deficit of about 29mm, which means that the crop is in short supply of water to reach its potential biomass (water stress on canopy = 1%). Consequently, the total water input for net irrigation simulation run shows a decrease in biomass of about 0.37ton/ha associated with a decline of only 0.14ton/ha in grain yield (Figure 11) that makes net irrigation expressing the highest water productivity coefficient (1.52kg yield/m3 evapotranspiration) compared to both practiced (applied) and simulated gross irrigation water productivity (1.5 and 1.49, respectively).

Figure 8. Soil water balance (using average for stages)

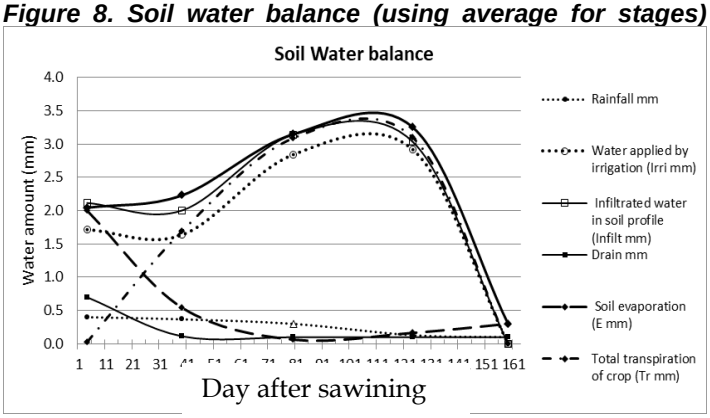

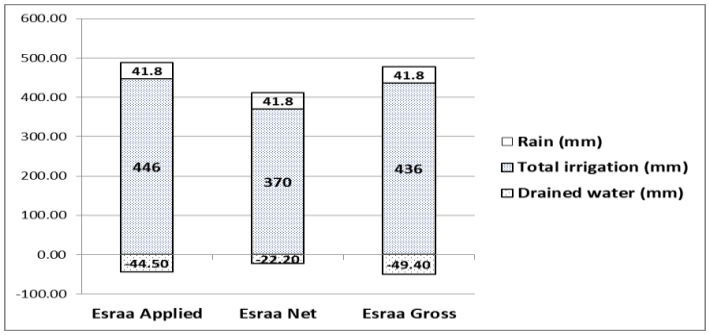

Figure 9. The cumulative water inputs

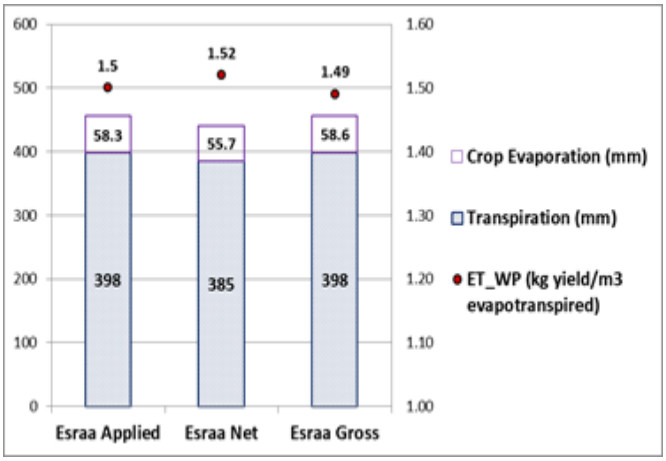

Figure 10. Cumulative crop water needs

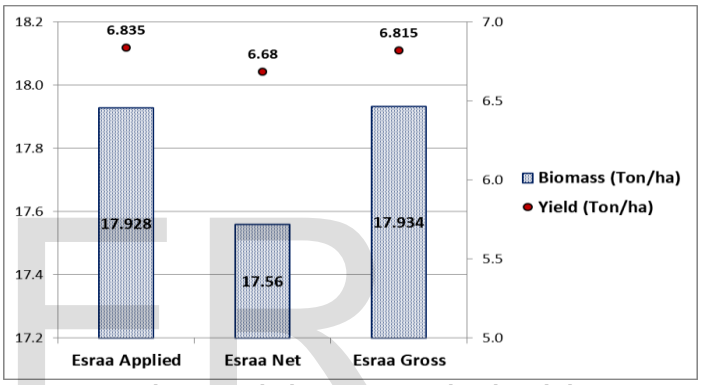

Figure 11. The cumulative crop production (Biomass and grain yield).

3.3.2. Testing the local calibrated model along a temperature gradient and with other comparable local climates

The simulation runs were done for a set of enforced temperature gradient inputs of five degrees Celsius below and above normal climate status, with steps of one degree negative or positive increments, to test the consistency in their cumulative outputs. Consequently, although the biomass increases with the increasing air temperature at the negative side of the temperature gradient reaching slightly higher than that of normal climate, it steeply declined at the positive side of the gradient (Figure 12). A similar trend of change is found for water productivity of evapotranspiration, which controls biomass production, but with the steep increase at the negative side followed by a lower decline at the positive side. Meanwhile, the grain yields show more regular responses to change in air temperature with balanced increases and decreases at the negative and positive sides of the temperature gradient. Nevertheless, the reached harvest indices that control the amount of grain yield shows a steep increase in values at the negative side up to the status of normal climate then slightly oscillates

above and below this status at the positive side of the temperature gradient.

The level of association between the values of each of biomass, grain yield, reached harvest indices, and water productivity for cumulative biomass production (Figure 13) reveal the rational high significant association (R^2 = 0.99) between the biomass production and water productivity for biomass (ETc-WP), hence crop's evapotranspiration. The wider variance in higher than normal temperature values results in the insignificant association (R^2 = -0.08) between biomass water productivity and the grain yield, which reflects the insignificant association (R^2 = 0.11) between the reached percentages of harvest indices and biomass water productivity.

Apparently, under the proposed assumption for these experimental simulations, the longer is the crop cycle for the stepwise decrease in temperature (negative side of images) compared to normal temperature status the larger is the amount of soil water content at vegetative and early flowering stages (with longer flowering and shorter grain filling stages) with progressing increments exceeding soil field capacity and hence draining. This arrangement is associated with a notable trend of decline in biomass and hence grain yield.

Figure 12. Cumulative simulation output values for enforced temperature gradient inputs of five degrees Celsius below and above normal climate status.

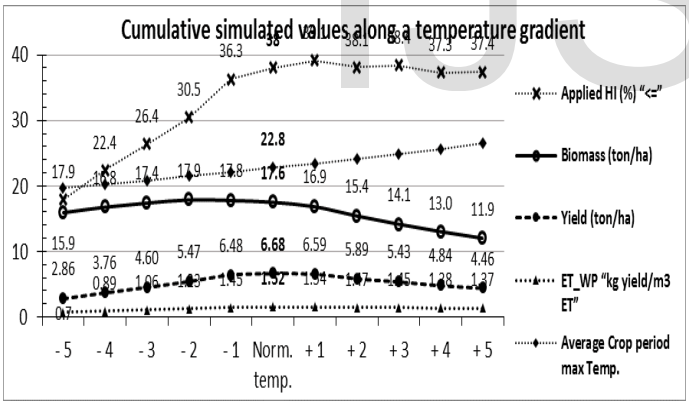

Figure 13. The levels of association between the values of each of biomass, grain yield, reached harvest indices and the values of biomass's water productivity.

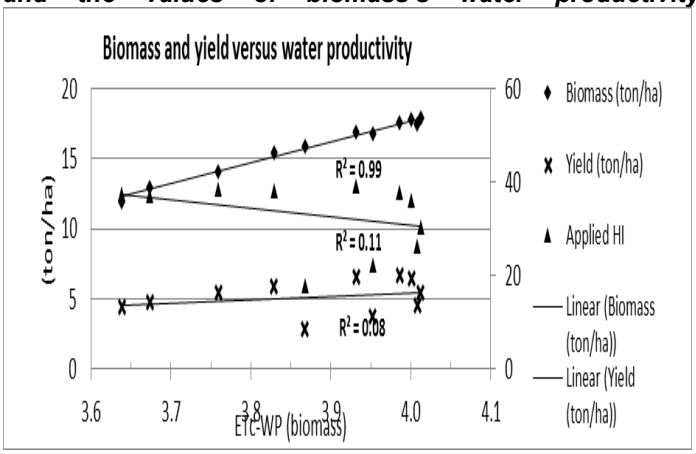

4. DISCUSSION

Model calibration involved using the verified calibrated values of specific parameters and controls in addition to phenology from field observations and measures and under no deficiencies of macronutrients (N, P, and K) that could alter a number of the conservative parameters in AquaCrop model (Andarzian et. al. 2011; Vanuytrecht et. al. 2013; Raes et al. 2016). Climate data using long term (20 years) average of metrological elements for the nearest stations were produced using the FAO, New LocClim program. These data sets are required as driving input to the crop and irrigation models used in the present study observed results have been used to calibrate AquaCrop model parameters at the different growth stages.

Combinations of crop coefficients (Kc) were tried as input to CROPWAT program to set the corresponding irrigation schedule, which is then used as input to AquaCrop model to calibrate Kc parameter by the values resulting in the least amount of needed irrigation water that produces acceptable yield performance compared to field measures. Several iterations were accomplished for each crop stage. For example, the highest yield (6.941 ton/ha) has been obtained calibrating Kc initial stage as 0.3 after calibrating Kc of mid-season and late season to 1.7 & 0.25 respectively, yet it is associated with the greatest value of water stress on canopy expansion (13%). While the selected least irrigation amount that produced an acceptable yield (6.680 ton/ha) has been obtained calibrating Kc to 0.5 for the initial stage. Accordingly, the calibrated combination of crop coefficients (Kc: 0.5, 1.07, 0.25) has been used to evaluate irrigation needs, and when applied in the model the crop uses 369.9 mm irrigation water producing 6.680 ton/ha grains yield associated with low moisture stress. The

calculated value of grain yield per total biomass (air dry weight) percentage from field measurements are used to calibrate the model input for harvest index (HI), while maximum grains weight is used to verify model's simulation output for yield production.

Using the local calibrated *AquaCrop* model in this study to evaluate its capability of responding to climate change scenarios, as one of the intended objectives, requires additional confirmation actions. One of which is to test how the complex model algorithm performs along a set of enforced temperature gradients through five degrees Celsius below and above normal climate status, with one degree negative or positive increments, while using the same irrigation quantity and schedule applied for normal climate case.

Another validation action is to run a simulation test to check the equity of the model for experimentation with proposed climate scenarios in this study using diverse extracted climate normal data of local sites have similar conditions in newly reclaimed areas, the previous two validation simulation tests reassure the practical intellectual hint of using the local calibrated AquaCrop model in this study for virtual experimentation. Indeed, several researchers used AquaCrop model to investigate the impact of climate change on wheat crop yield using diverse methods of experimentation methodologies

The present study has implemented six simulation runs of AquaCrop model to represent the different modified climate files (temperature, ETo and rainfall) which hypothesize selected projected climate change scenarios. Those cover situations of high climate with double rain, high climate with normal rain, high climate with zero rain, low climate with one-half rain, low climate with normal rain, and low climate with double rain. These scenarios change the wheat crop cycle from 152 days accumulating growing degree days (GDD) of 2411°C for normal climate to 137 days for the high climate and 166 days for the low climate scenarios' sets, which accumulates almost similar 'GDD' values (2393 & 2395°C respectively). A gap of twenty-nine days is needed to compensate for temperature difference per day among the two scenarios.

The relationship between simulated crop biomass production under the hypothesized climate scenarios and the driving variables used by AquaCrop model is tested by applying stepwise multiple regression. The predicted regression equation with the highest coefficient of determination (R^2 = 0.999) and arranged according to probability significance is stated as follows: {Biomass (Ton/ha) = 4.2402 + 0.0413 X [Transpiration mm] -1.0751 X [ETc-WP] -0.0162 X [Crop cycle soil evaporation]}. Focusing on all information and analyses acknowledged in the present study can help in exploring the AquaCrop model's capability of predicting the required measures for reconciliation of the impacts of climate change scenarios regarding the wheat crop planted in the selected pilot site and to test the needs and consequences to mitigate the impacts of climate change by taking fine-tuning measures to resolve the same previous hypothesized scenarios. The primary changing variable for these hypothesized scenarios has been changing temperature values (modifying ETo) and amount of rainfall, hence the indirect impacts of temperature regimes on crop water balance and potential productivity.

5. CONCLUSION

Newly reclaimed areas in northern Egypt (Nile Delta fringe deserts) are confronted by the heterogeneity in environmental variables especially inland physiognomy, topography, soil characteristics, and agro-climate conditions at microscale spatial levels. This should be considered when evaluating the impacts of the climate change phenomenon on agroecosystems. The temporal and spatial variability in calibrated soil characters in newly reclaimed marginal land areas could be major driving factors for predicting the response to mitigate varied climate change impacts rather than the calibrated crop cultivars parameters.

Optimizing the amount and schedule of irrigation water in response to climate change conditions has been realized by adopting a new approach related to the deficit irrigation strategy; working at microscale spatial level by handling programmatically combined interactive runs of AquaCrop and CROPWAT programs, testing the equity of the model for experimentation with proposed climate scenarios in the present study firstly through enforced temperature gradient (-5 to +5°C) and secondly by using diverse extracted climate normal data of local site reassured the intellectual hint of using the local calibrated AquaCrop model in the present study for virtual experimentation. According to the enforced temperature gradient simulation test output statistics it could be advised that biomass water productivity, reflecting crop's maximum biomass water use efficiency, could be considered as a reliable reference indicator for evaluating the efficiency of crop's irrigation scheme. While, an added value of using diverse extracted climate normal data of local sites simulation test provides a good example to suggest applying locally calibrated models at microscale spatial level in Mediterranean regions.

Finally, the achieved experience of this research project highlights the necessity of using smart agriculture tools and models for setting on-site scheduling of irrigation water that produces actual soil water availability rank versus climate conditions, which would be the ultimate control of both saving water and producing acceptable values of biomass and yield subject to anticipated climate change incidence, which is much more appreciate in Mediterranean land regions.

REFERENCES

1. Andarzian, B., Bannyan, M., Steduto, P., Mazraeh, H., Barati, M.E., Rhnama, A. (2011). Validation and testing of the AquaCrop model under full and deficit irrigated wheat production in Iran, Agric. Water Manage., 100: 1-8.
2. CROPWAT Software, FAO, Land and Water Division. 2018. Available online: http://www.fao.org/landwater/databases-and-software/cropwat/en/ (accessed on 20 april 2020).
3. CSA, FAO 2010: "Climate-Smart" Agriculture, Policies, Practices and Financing for Food Security, Adaptation and Mitigation, FAO, 2010
4. Doorenbos, J. and Kassam, A.H. (1979) Yield response to water. FAO Irrigation and Drainage, Paper 33, Rome, 193 p
5. FAO (Food and Agriculture Organization of the United Nations) (2009) Climate change implications for fisheries and aquaculture 2009. Food and Agriculture Organisation, Rome, p 212
6. FAO. 2010. Climate-smart Agriculture Sourcebook. Rome. Available at www. fao.org/docrep/018/i3325e/i3325e.pdf
7. FAO (2010b) Climate smart agriculture: policies, practices and financing for food security, adaptation and mitigation, Rome
8. FAO. Water for Sustainable Food and Agriculture. A Report Produced for the G20 Presidency of Germany; Food and Agriculture Organization of the United Nations: Rome, Italy, 2017.
9. Food and Agriculture Organization of the UN (FAO) (2018b), Aquastat Main Database, http://www.fao.org/nr/water/aquastat/data/query/index.html?lang=en.
10. Garcìa-Mollá, M., Sanchis-Ibor, C., Ortega-Reig, M. V. and Avellá-Reus, L. 2013. Irrigation associations coping with drought: The case of four irrigation districts in eastern spain. In K. Schwabe, J. Albiac, J. D. Connor, R. Hassan and L. M. González., eds. Drought in Arid and Semi-Arid Regions: A Multi-Disciplinary and Cross-Country Perspective, pp. 101–122. doi: 10.1007/978-94-007-6636-5_6.
11. Iqbal, M.A., Shen, Y., Stricevic, R., Pei, H., Sun, H., Amiri, E., Penas, A., Rio, S. del., (2014). Evaluation of the FAO AquaCrop model for winter wheat on the North China Plain under deficit irrigation from field experiment to regional yield simulation. Agric. Water Manage. 135:61–72.
12. J. Grieser, R. Gommes, M. Bernardi 2006 New LocClim - the Local Climate Estimator of FAO, https://www.researchgate.net/publication/288879070_New_LocClim-the_local_climate_estimator_of_FAO
13. McGill, J., Prikhodko, D., Sterk, B., & Talks, P. (2015). Egypt: Wheat sector review. Rome: Food and Agricultural Organization of the United Nations.
14. Merrian, JL, Shearer MN, Burt CM (1980). Evaluating irrigation systems and practices. In: Design and Operation of Farm Irrigation Systems. Edited by Jensen ME and St. Joseph (Mich: ASAE) 721-760.
15. Mkhabela, M.S., and Bullock, P.R. (2012). Performance of the FAO AquaCrop model for wheat grain yield and soil moisture, Agric. Water Manage., 110: 16-24.
16. Singh, A., Saha, S., Mondal, S. (2013) Modelling irrigated wheat production using the FAO AquaCrop model in West Bengal, India for Sustainable Agriculture. Irrig. Drain., 62: 50-56.
17. Tedeschi, A., Hamminga, W., Postiglione, L., & Menenti, M. (1995). Sustainable irrigation scheduling: effects of saline water on soil physical properties. In *ICID/FAO workshop; irrigation scheduling: from theory to practice. Rome, ICID, 1995, Background Doc. 10*
18. Vanuytrecht E, Raes D, Willems P. 2014. Global sensitivity analysis of yield output from the water productivity model. Environmental Modelling & Software, 51, 323–332
19. Wally & Verdonk, (2016) The State and Development of Aquaculture in Egypt, https://apps.fas.usda.gov/newgainapi/api/report/downloadreportbyfilename?filename=The%20State%20and%20Development%20of%20Aquaculture%20in%20Egypt%20_Cairo_Egypt_11-6-2016.pdf
20. Wiebe, K., Lotze-Campen, H., Sands, R., Tabeau, A., Mensbrugghe, D. van der, Anne Biewald, Bodirsky, B., Islam, S., Kavallari, A., Mason-D'Croz, D., Christoph Müller, Popp, A., Robertson, R., Robinson, S., Meijl, H. van, Willenbockel, D., 2015. Climate change impacts on agriculture in 2050 under a range of plausible socioeconomic and emissions scenarios. Environ. Res. Lett. 10, 085010. https://doi.org/10.1088/1748-9326/10/8/085010